

UNDERSTANDING LUNAR OLIVINE COMPOSITION OF A PART OF OCEANUS PROCELLARUM USING TERRESTRIAL ANALOGUES. N. Chaudhuri¹, K.N. Kusuma¹ and S. A. Bharathvaj¹; ¹Department of Earth Sciences, Pondicherry University, Puducherry, India, 605014. (nabamitach93@gmail.com)

Introduction: Olivine is one of the common minerals found in lunar basalts and have been widely reported from the lunar surface. The presence of olivine is majorly attributed to exhumation during impacts and can be associated to lunar mantle [1, 2, 3, 4]. In recent studies, olivine is reported even within smaller craters where complete crustal exhumation is not feasible [5]. Olivine is one of the earliest minerals to crystallize and its geochemistry can provide insight to evolutionary stages of lunar lithology.

The electronic transitions in the Fe²⁺ causes three absorptions in the olivine spectra near 1000 nm, two exterior absorptions because of Fe²⁺ in M1 site and one interior absorption due to Fe²⁺ in M2 site [6, 7, 8, 9]. The M1 site related absorption is around 850 nm and 1250 nm, whereas the M2 site related absorption is centred around 1050 nm. The absorption position of olivine shifts toward the longer wavelength with increasing iron content [6, 9]. In this work, we attempt to characterize the lunar olivine spectra with the aid of the olivine composition of terrestrial analogues.

Datasets and Methodology: We have studied a part of the Oceanus Procellarum region which hosts a variety of basalts. Moon Mineralogy Mapper (M³) reflectance datasets were processed for compositional analysis.

Analogue samples. For analogue analysis, we have used four dunite samples collected from Tamil Nadu Magnesite Mines (TANMAG), India and four olivine samples (<60 μm grain size) from the USGS Digital Spectral library [13], displaying a range of composition. The unaltered dunite samples of TANMAG were powdered for obtaining major element oxides by XRF analysis and VNIR-reflectance spectra. The elemental information was further used to derive the molar Mg# using the following formula.

$$\text{Mg\#} = \frac{\text{Mg}}{(\text{Mg} + \text{Fe})}$$

M³ Analysis: Integrated Band Depth (IBD) analysis allows identification of diverse mineral species on the lunar surface using M³[10, 11, 12]. IBD1000 and IBD2000 was used to characterize lunar mafic lithology; and IBD1250 was used to highlight the anorthosite [10, 11, 12]. The color composite images were derived by assigning IBD1000, IBD2000 and IBD1250 to red, green and blue channels respectively to highlight lithological variations.

Modified Gaussian Model (MGM). Modified Gaussian model is a deconvolution technique which resolves overlapping absorption Gaussians into its

corresponding individual end members [14, 15]. We have attempted MGM-deconvolution on a M³ spectra to derive individual absorption bands of olivine (Table 1) and parameters were used to find the composition of olivine in the analyzed M³ spectra (Table 2).

Results: The IBD colour composite image highlights the lithological variations amongst the basalts depicted by the various hues of the image (Figure.1). The region is dominated by pyroxene, but presence of red indicates a significant occurrence of olivine. The pixel size of M³ reflectance dataset will exhibit a spectrum representing mixed mineralogies. To understand the composition of lunar olivine, MGM based deconvolved band center at 1000 nm can be used in synergy with the analogue samples having for comparable band centers. With increase in iron content (low Mg# value), the absorption position of olivine shifts toward the longer wavelength [6, 9], the shift becomes more pronounced for lower Mg# range (Figure.2). The M³-olivine spectra used for MGM deconvolution in this study is truncated at 1600 nm to avoid interferences induced by Cr-spinel related features [16, 17, 18]. The derived band centres indicate that the absorption band due to Fe²⁺ in the in M1 site is at 829 and 1301 nm, whereas the M2 site related absorption is at 1048 nm (Figure.3, Table 2). From Figure 2, the corresponding composition for the 1048 nm absorption centre shows an Mg#>0.8. The observed absorption band centers at shorter wavelength (hence a higher Mg#), can be an indication of a primitive basalt source [19].

Ongoing Work: The presence of the exterior M1 absorption beyond 1300 nm hints presence of other minerals such as pyroxene in the analyzed M³ spectra. Observations from other varieties of lunar olivine spectra in the region will provide more insight to the evolution of the basalts. We are currently working on more lunar spectra of the olivine and other analogue samples from for better MGM-derived solutions. The higher spectral resolution of the laboratory spectra will help us to better understand the compositions and mineralogy which can be extended to lunar studies.

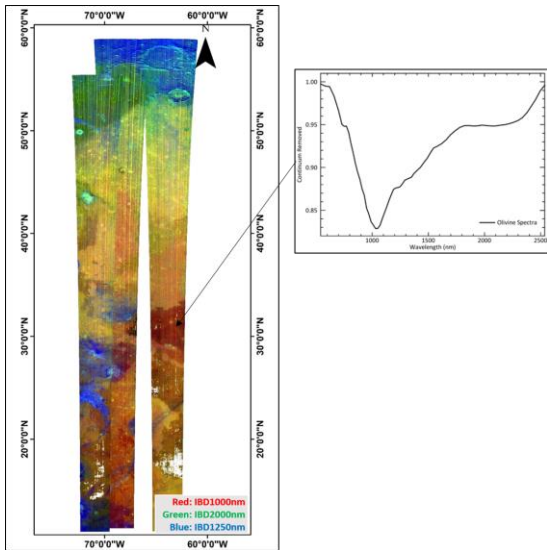


Figure 1: IBD color composite image derived from M^3 image of the Oceanus Procellarum region. The region is predominantly basaltic. The range in the shades of the colour indicates the variations in the mafic lithologies. The continuum-removed reflectance spectra acquired from one of the basaltic units show presence of olivine.

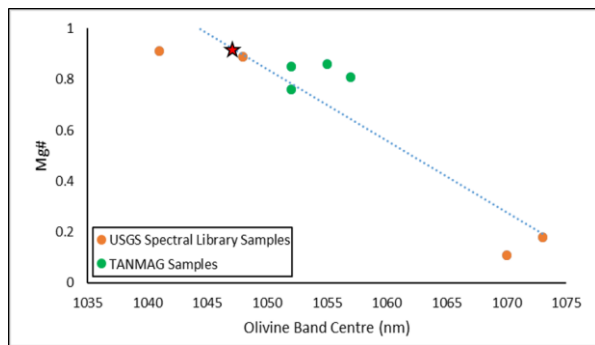


Figure 2: Plot of Mg# vs the absorption band centre of olivine for the terrestrial analogue samples. The USGS spectral library samples extend the range of Mg# helping our understanding of band centres for highly forsteritic or fayalitic olivines. The red star represents the 1050-nm associated MGM-deconvolved gaussian of the M^3 olivine spectra.

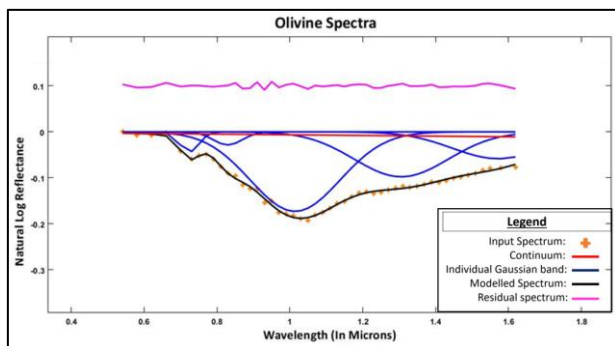


Figure 3: MGM derived gaussians for an M^3 spectra for an olivine in the Oceanus Procellarum region.

Table 1. Starting model parameters for MGM deconvolution for Olivine spectra taken from M^3 reflectance dataset.

Band	Centre	FWHM	Strength
1	700±200	300±200	-0.03±200
2	850±200	300±200	-0.05±100
3	1050±200	500±400	-0.10±400
4	1200±200	500±400	-0.05±400
5	1600±400	500±400	-0.03±400

Table 2. Final model parameters for MGM deconvolution for Olivine spectra taken from M^3 reflectance dataset.

Band	Centre	FWHM	Strength
1	724	61.507258	-0.044
2	829	94.6768942	-0.029
3	1048	285.269571	-0.170
4	1301	313.34173	-0.098
5	1570	306.234542	-0.057

Current RMS error = 3.808156e-03

References: [1] Pieters, C. M. (1982) *Science*, 215(4528), 59-61.; [2] Pinet, P. C. et al (1993) *Science*, 260(5109), 797-801.; [3] Yamamoto, S. et al (2010). *Nature Geoscience*, 3(8), 533-536.; [4] Melosh, H. J. et al. (2017) *Geology*, 45(12), 1063-1066. [5] Li, H. et al (2023). *Icarus*, 391, 115333. [6] Burns, R. G. (1970). *American Mineralogist: Journal of Earth and Planetary Materials*, 55(9-10), 1608-1632. [7] Burns, R. G. (1972). *Chemical Geology*, 9(1-4), 67-73. [8] Burns, R. G. (1974). *American Mineralogist: Journal of Earth and Planetary Materials*, 59(5-6), 625-629. [9] Burns, R. G (1993). *Cambridge university press*. [10] Mustard, J. F. et al (2011). *JGR:Planets*, 116(E6).[11] Besse, S. et al (2011). *JGR:Planets*, 116(E6).[12] Cheek, L. C. et al (2013). *JGR:Planets*, 118(9), 1805-1820.[13] Clark et. al. (2003) *USGS, Open File Report 03-395*. [14] Sunshine, J.M. (1990) *JGR Research*, 93, 6955-6966.[15] Sunshine, J.M. and Pieters, C.M. (1993) *JGR*, 98, 9075-9087.[16] Isaacson, P.J. et al (2011) *JGR:Planets*, 116(E6).[17] King, T. V., & Ridley, W. I. (1987). *JGR:Solid Earth*, 92(B11), 11457-11469. [18] Cloutis, E. A. et al (2004). *Meteoritics & Planetary Science*, 39(4), 545-565. [19] Basaltic Volcanism Study Project (BVSP) (1981).